POAC'25
St. John's, Newfoundland and Labrador, Canada

Proceedings of the 28th International Conference on Port and Ocean Engineering under Arctic Conditions
Jul 13-17, 2025
St. John's, Newfoundland and Labrador
Canada

Validation of Time History Model of a Ship Ice Collision for Spherical Cap Shaped Ice Samples

Edward J.D. Bryson[1], Sthéfano L. Andrade [1], Bruce W.T. Quinton[1]
[1] Memorial University of Newfoundland, St. John's, NL, Canada

ABSTRACT

In its simplest form, the Popov-Daley model is an energy-based method used for calculating ship-ice collision forces by deriving an effective kinetic energy of a ship-ice impact which is dissipated into ice crushing energy. This model is not only the current basis for design ice loads in the International Association of Classification Societies (IACS) Unified Requirements for Polar Class Ships (Polar URs) but also finds application in multiple areas of academic interest, from safe speed studies involving both ice strengthened and non-ice strengthened ships to its application in computer programs when simulating ice loads. In some instances, such as during the analysis of moving loads or during the development of progressively growing load patches for use in finite element simulations, knowing how the impact force grows over a period of time is necessary. An analytically derived solution for the time history of a Popov-Daley ship-ice collision exists and has been preliminarily validated using data from double pendulum impact tests comprising of a rigid panel and cone shaped ice samples. This study details further validation work completed by analyzing impact data from two additional double pendulum tests where approximately spherical cap shaped ice samples were used. Nominal pressure-area curves derived from the impact data were used in conjunction with the impact velocity, ice geometry, and effective mass of the collision system to model the relationship between ice indentation depth and time over the course of the completed impact tests. The results were validated against visual data of the impacts recorded with high-speed cameras. The applicability of the process pressure-area method for spherical cap ice geometries is discussed.

KEY WORDS: Double Pendulum Experiment; Popov Method; Ship-Ice Impact Mechanics; Ship-Ice Impact Time History; Ship-Ice Interaction.

INTRODUCTION

The International Classification Society's (IACS) Unified Requirements for Polar Class Ships, or Polar URs (IACS, 2019), were developed in the 1990s as part of an effort to unify many preexisting ice class rules into one regime through which vessels operating in polar waters are classed (Riska and Kamarainen, 2012) and have since been gradually accepted as the industry standard (Kim and Amdahl, 2016). First introduced in the Polar URs as part of the design ice load model, the Popov-Daley method (Daley, 2000) is used for calculating ship-ice impact forces. It is analytically based on a balance of the available kinetic energy of a ship-ice collision scenario and the indentation energy expressed either solely through ice crushing, which is the assumption used in the Polar URs, or as a combination of ice crushing and structural indentation energies. The Popov-Daley method has since been used in numerous academic studies and assumptions made during its original application in the Polar URs have been revisited to allow for consideration of scenarios relevant to both icebreaking hull forms and non-ice-strengthened ships (Daley, 2015; Daley et al., 2017; Daley and Kim, 2010; Daley and Liu, 2010; Dolny, 2016; Lande Andrade et al., 2022). This includes consideration of finite ice floes and deformable hull structures.

The increasingly broad application of the Popov-Daley method also includes scenarios where the time history of the ice impact may be of interest. For example, the development of a progressive load patch based on a Polar URs design ice load (Lande Andrade et al., 2022) applies a Popov-Daley style load over a period of time. This and other past studies involving the Popov-Daley method have either calculated the time history of the collision using numerical methods, assumed the collision time to be instantaneous, or have ignored it entirely. Recently, an analytical solution for the time history of a Popov-Daley style ship ice impact has been derived directly from the underlying energy equality using the Polar URs based assumptions (Bryson et al., 2025). This model was validated against existing numerical methods and a large double pendulum experiment using a cone shaped ice sample with promising results. This study presents additional validation work using double pendulum experiment results of ice samples with a spherical cap geometry.

THE POPOV-DALEY METHOD

Energy methods for the evaluation of ice loads on ships were first developed in the 1960s (Popov et al., 1967) where a collision between a ship and ice, each unrestrained with motions in six degrees of freedom, is reduced to a single degree of freedom impact in the direction normal to the contact plane. The effective kinetic energy of the collision is calculated using equation (1).

$$KE_e = \frac{1}{2} M_e {V_n}^2 \tag{1}$$

Where M_e is the effective mass of the ship ice system and V_n is the impact velocity each in the normal direction of indentation. The calculation of the effective mass differs depending on the collision scenario assumptions. Detailed calculations for M_e as used the Polar URs is

presented in the appendix of Daley (1999), where the ice is assumed to be semi –infinite, whereas a more general version considering a finite ice floe can be found in Dolny (2017).

The calculated available kinetic energy is converted into indentation energy which in the case of the Polar URs is comprised solely of ice crushing energy. A "process" pressure area relationship characterizing the ice crushing strength was applied by Daley (1999) which expresses the ice indentation energies and forces as a function of the normal indentation depth. Average ice pressure is represented as a function of the contact area, and a closed form solution of the collision force as a function of solely the indentation depth can be derived. The average pressure is calculated as follows:

$$P_{av} = P_o \cdot A^{ex} \tag{2}$$

Where P_{av} is the average contact pressure, P_o is the nominal average pressure at a contact area of $1\ m^2$ which in the Polar URs is taken as a class based constant, A is the contact area, and ex is the ice exponent, also taken as a constant. The contact force F_n is found by multiplying the pressure by the area:

$$F_n = P_{av} \cdot A = P_o \cdot A^{1+ex} \tag{3}$$

The contact area, A, is a function of the ice geometry and the normal indentation depth ζ_n. A variety of contact geometries have been introduced by Daley (1999) have are expressed in terms of shape factors such that the impact force may be expressed as follows:

$$F_n = P_o \cdot f_a \cdot {\zeta_n}^{f_x - 1} \tag{4}$$

Where f_a and f_x are the form factors and are a function of the contact geometry and the ice exponent ex. The ice indentation energy of the impact is derived from the force as follows:

$$IE_i = \int_0^{\zeta_n} F_n d\zeta \tag{5}$$

Therefore:

$$IE_i = \frac{P_o}{f_x} \cdot f_a \cdot {\zeta_n}^{f_x} \tag{6}$$

By equating equations (1) and (6), a relationship between the energy of the ship ice collision system and total indentation depth of crushed ice is found.

Time History Model

Bryson et al. (2025) presented a solution for the relationship between the normal indentation depth and time of a Popov-Daley style collision derived directly from the kinetic – indentation energy equality. Assuming a rigid hull, at any point in time during the impact the ice indentation energy is equal to the reduction in kinetic energy.

$$IE_i(\zeta_n) = KE_e - KE(\zeta_n) \tag{7}$$

This may be resolved into a relationship between the collision time and the indentation depth per Bryson et al. (2025) as follows.

$$t(\zeta_n) = \frac{\zeta_n \cdot {}_2F_1\left(\frac{1}{2}, \frac{1}{fx}; \frac{fx+1}{fx}; \frac{2 \cdot P_o \cdot f_a \cdot {\zeta_n}^{fx}}{{V_o}^2 \cdot f_x \cdot M_e}\right)}{V_o} \tag{8}$$

Where equation (8) represents a solution to the indentation-time relationship from $0 \leq \zeta_n < \zeta_{max}$. At a penetration depth of ζ_{max}, where the collision is assumed to end, the ordinary hypergeometric function present in the solution has the following form:

$${}_2F_1(\alpha; \beta; \gamma; 1) \tag{9}$$

This is a special case and leads to the following solution for the total time of the collision:

$$t_{total} = \frac{\sqrt{\pi} \cdot \sqrt[fx]{\frac{{V_o}^2 \cdot f_x \cdot M_e}{2 \cdot P_o \cdot f_a}} \cdot \Gamma\left(\frac{f_x+1}{f_x}\right)}{V_o \cdot \Gamma\left(\frac{1}{f_x} + \frac{1}{2}\right)} \tag{10}$$

The two models given in equations (8) and (10) have been validated against both numerical methods and experimental data of a double pendulum experiment using a conical ice sample (Bryson et al., 2025).

EXPERIMENTAL VALIDATION AGAINST SPHERICAL CAP ICE SAMPLES

The following validation work is completed using data from two large double pendulum experiments presented in a complimentary paper (Andrade et al., 2025). These experiments use spherical cap shaped ice samples, still images of which are shown in Figure 1. The geometries were hand carved, with the rougher shape of experiment 5 showing a first attempt at a technique which was later improved upon for experiment 8. Impact rebound was negligible, and thus the

collisions were assumed inelastic. Other details for these experiments are found in Andrade et al. (2025).

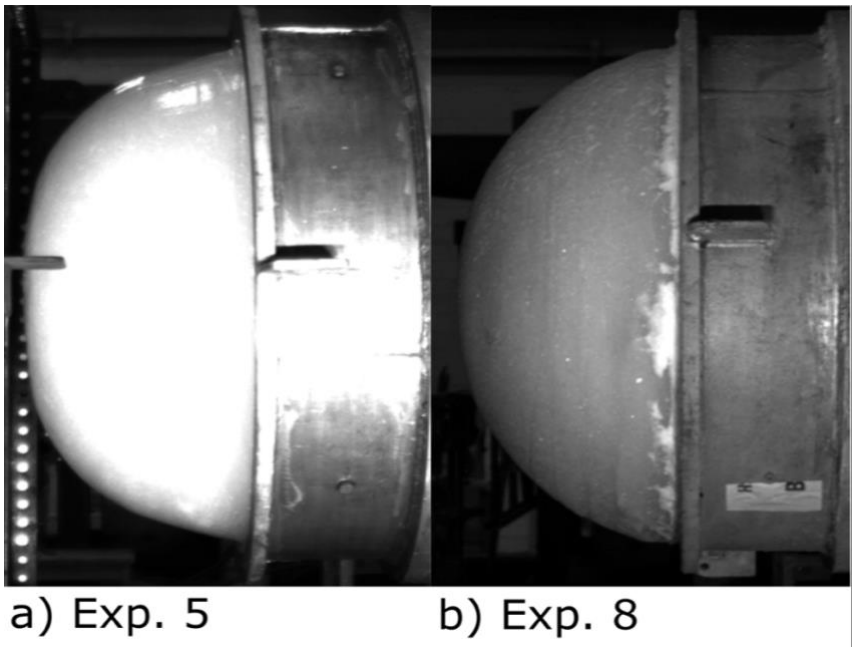

Figure 1: Still Images of the Spherical Cap Shaped Ice Samples.

The five inputs required by the time history models include the initial velocity in the normal direction of indentation V_o, the effective mass of the system M_e, the ice strength term P_o, and the form factors f_a and f_x. These values are found in the same manner as Bryson et al. (2025), with the impact velocity being determined through analysis of the high speed videos using digital image correlation (DIC) and the effective mass of the system found through use of the initial impact velocity and the effective kinetic energy $\mathrm{KE_e}$ per equation (1). Table 1 details the required carriage data needed to achieve this, with the initial impact velocity found to be 6.1 m/s for experiment 5 and 6.005 m/s for experiment 8. Consequently, the effective mass is 2,393.0 kg for experiment 5 and 2,393.0 kg for experiment 8. Figure 2 shows the indentation – time relationships as measured from the high-speed cameras and the DIC software.

Table 1: Ice and Panel Carriage Data for Experiments 5 and 8.

Carriage Data		*Mass*	*Measured Drop Angle*	*Theoretical Impact Speed*	*DIC Impact Speed*	*Theoretical Kinetic Energy*	*DIC Kinetic Energy*
		kg	degree	m/s	m/s	J	J
Exp 5	Ice carriage	5,214.8	40.65	3.076	3.016	22,774.5	21,889.4
	Panel carriage	5,161.6	40.4	3.058	3.084	22,258.0	22,632.4
	Total	----	----		6.100	45,032.5	44,521.8
Exp 8	Ice carriage	5,214.8	40.4	3.058	3.005	22,506.9	21,731.5
	Panel carriage	5,161.6	40.4	3.058	3.000	22,258.0	21,414.0
	Total	----	----	6.117	6.005	44,764.9	43,145.5

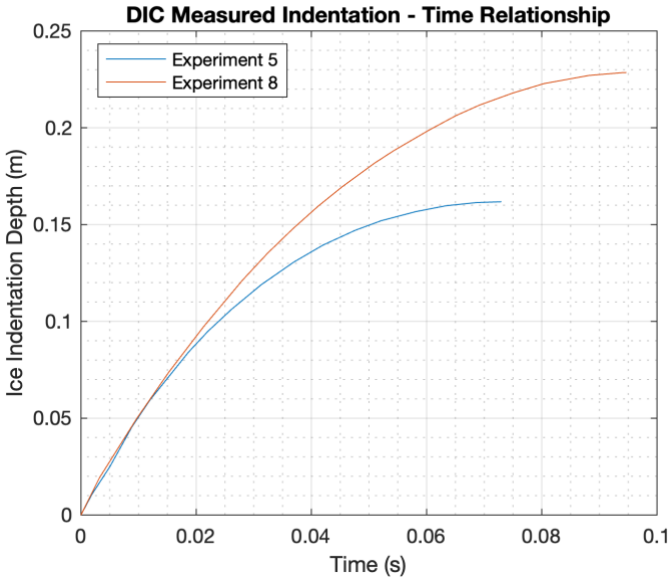

Figure 2: DIC Measured Ice Indentation vs. Time Relationship of Experiments 5 and 8.

Determination of the remaining terms requires fitting regressions of the nominal process pressure-area power curves described previously and defined in equation (2). This is done by calculating a nominal ice pressure as a function of the indentation depth using the impact load data in conjunction with the DIC measured ice indentation and an area indentation relationship based on the ice sample's nominal contact geometry. The ice strength term P_o is found directly from the power curve fit, and the form factors f_a and f_x are functions of the nominal contact geometry as well as the ice exponent ex, the second parameter of the pressure area curve.

Development of Process Pressure-Area Curves from Experimental Data

An area indentation relationship for spherical cap ice sample has been developed by Daley (1999) and is characterized by the following form factors.

$$fa = (2\pi R)^{1+ex} \tag{11}$$

$$fx = 2 + ex \tag{12}$$

Where R is the radius of an assumed circle from which the spherical cap ice sample is taken. This radius may be determined through analysis of the still images given in Figure 1, where the base of the ice sample is known to have a radius r of one metre. The indentation depth ζ_h associated with an assumed cross section of the sphere taken at the base of the ice sample may

be used to determine the radius R of the assumed sphere. This is done by considering the right-angle triangle formed by the radius of the cross section, r, the radius of the sphere, R, and the difference of the sphere radius and the indentation depth, $R - \zeta_h$. This is illustrated in Figure 3.

$$R^2 = (R - \zeta_h)^2 + r^2 \tag{13}$$

$$R = \frac{r^2 + {\zeta_h}^2}{2\zeta_h} \tag{14}$$

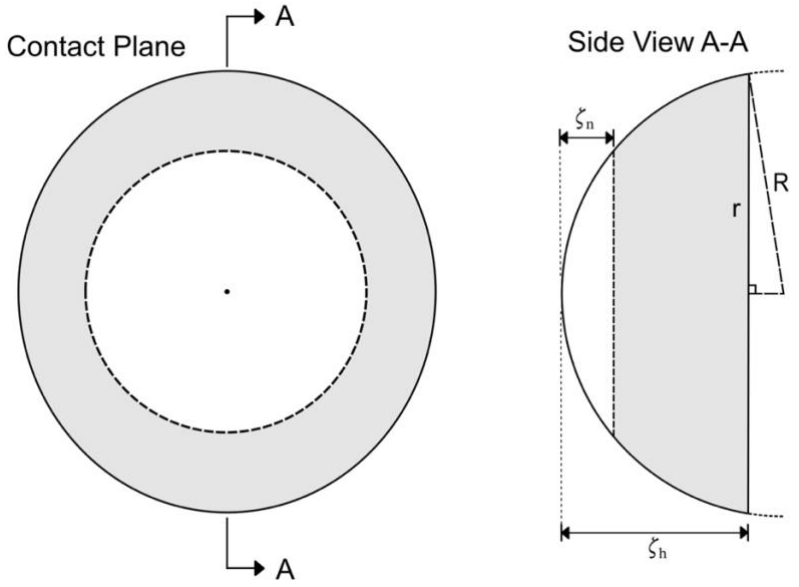

Figure 3: Spherical Cap Shaped Ice Specimen Geometry. The Grey Area Represents the Intact Ice at an Indentation Depth of ζ_n, ζ_h is the Depth of the Ice Sample, r is the Radius of the Sample Base, Assumed to be 0.5 m, and R is the Radius of the Ideal Sphere.

The calculated radii of the two assumed spheres from experiments 5 and 8 are equal to 0.580 m and 0.523 m respectively. In the same manner as Bryson et al. (2025), the impact is assumed to start based on the first significant increase in the load cell data, which is sampled at 100,000 Hz. The DIC camera data is sampled at 1,000 Hz and as such, it was assumed that the first visible indication of the impact on the high-speed camera corresponds to the 100th sampling of significant load cell data. This means that the calculated indentation depth from this first frame occurs at a collision time of 0.001 seconds and an indentation depth of 0 m is assumed at a collision time of 0 seconds. Linear interpolation was used cover the discrepancy in the sampling rates to allow comparison of the DIC displacement data and the load cell data. In this manner, the load data was used in conjunction with the calculated nominal contact area to develop the pressure-area data shown in Figure 4.

When fitting a power curve to the nominal pressure-area data in Bryson et al. (2025), the limitations of using an idealized relationship such as that introduced in equation (2) to represent the experimental data were acknowledged, including its use of an idealized crushing process with no spalling or other load shedding events. In addition, the real experimental data did not follow a general trend of decreasing nominal pressure for smaller contact areas and it should be noted that this is also the case for the spherical cap ice samples. As such, two methods for plotting the regression were tested. The first method, "Method 1", used all calculated pressure-area data to generate a rougher regression fit, while the second method, "Method 2", did not consider any data from smaller nominal contact areas that did not follow the same downward trend as the rest of the collision. One difference when applying Method 1 in Bryson et al. (2025) versus the present study is that the former used all collision data past a time of 0.001 in order to avoid using linearly interpolated displacement data from before the first frame of impact from the DIC data. This was acceptable for cone shaped ice samples as the nominal contact area is still relatively small at this point. With spherical caps however, the contact area grows significantly at the beginning of the collision and as such, all data starting at a collision time of 0 was used. Figure 4 shows the resulting regressions for all experiments using both methods. The regression parameter P_o is taken directly for use in the indentation time models and ex is used to determine fa and fx as per equations (11) and (12). Resultant time history model terms are summarized in Table 2.

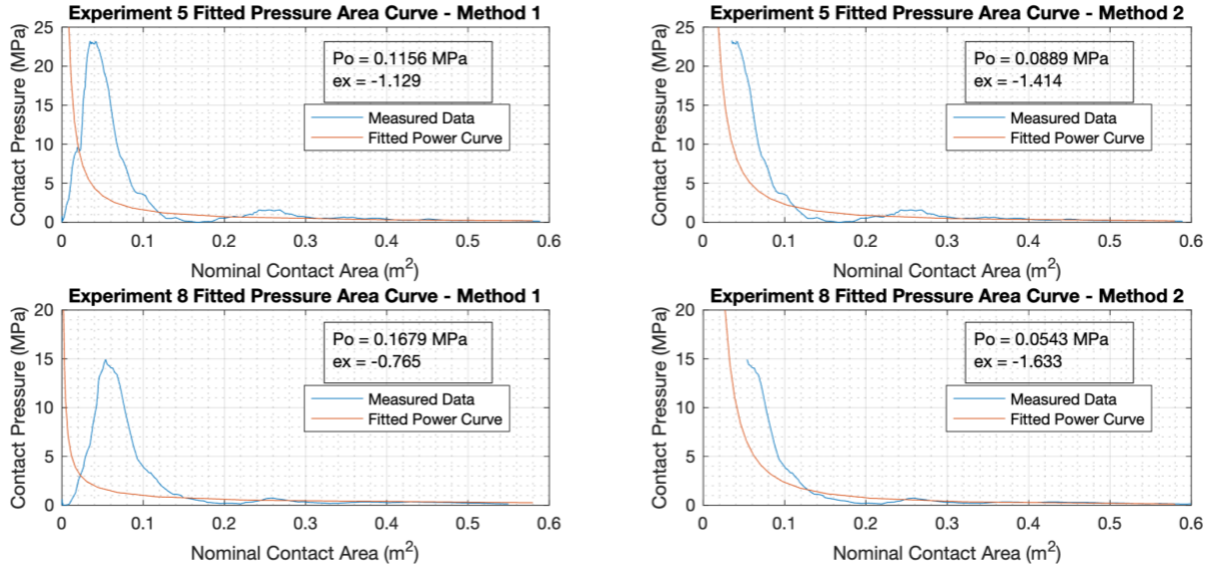

Figure 4: Fitted Power Curves using Methods 1 and 2 for Experiments 5 and 8.

Table 2: Calculated Time History Model Terms for Experiments 5 and 8.

	Initial Velocity V_o	*Effective Mass* M_e	*Ice Strength Term* P_o		*Form Factor* fa		*Form Factor* fx	
	m/s	kg	MPa		----		----	
	----	----	Mtd 1	Mtd 2	Mtd 1	Mtd 2	Mtd 1	Mtd 2
Exp 5	6.100	2,393.0	0.1156	0.0889	0.846	0.586	0.871	0.586
Exp 8	6.005	2,393.0	0.1679	0.0543	1.323	0.471	1.235	0.367

Validation Results and Discussion

Per both the Popov-Daley method and the indentation-time model assumptions, the end of the collision occur at the point of maximum indentation depth and no consideration is given to the forces and time duration of the unloading process. Figure 5 compares the measured DIC data with the time indentation model using parameters from both Method 1 and 2, and Table *3* summarizes the results.

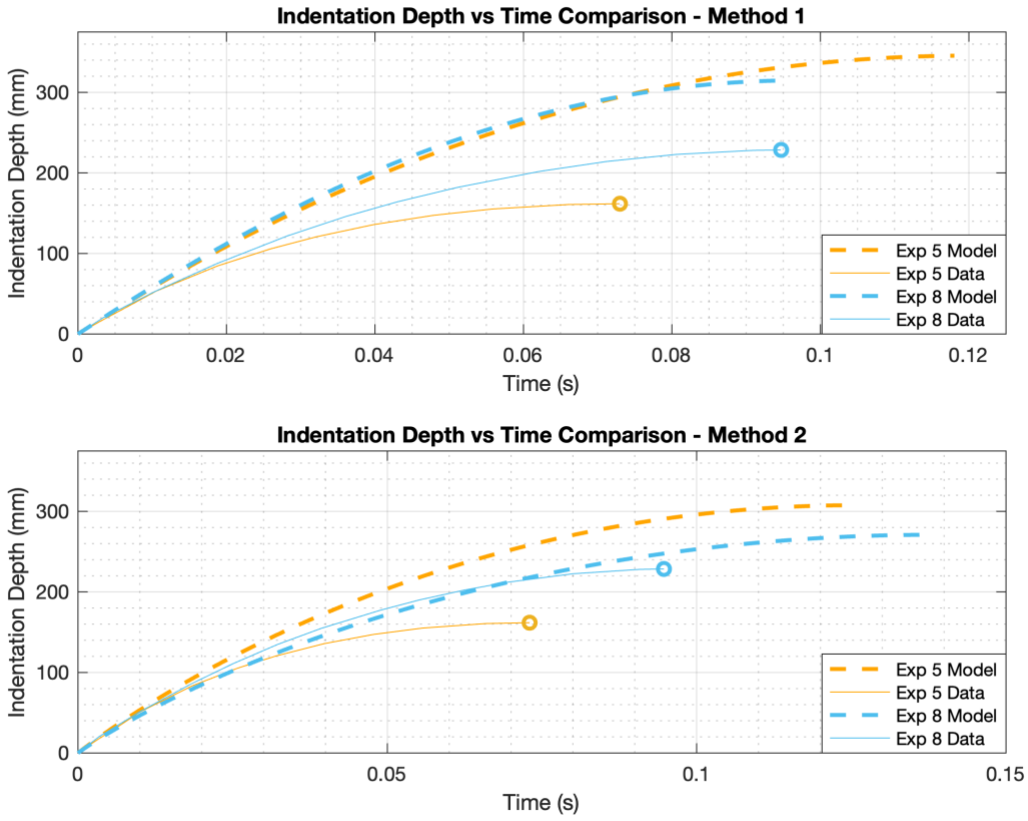

Figure 5: Comparison of Indentation Time Model with Experimental Results using both Methods for Determining Model Parameters.

Table 3: Comparison of Predicted and Actual Total Time and Total Indentation Depth Results for Experiments 5 and 8.

	Total Impact Time (Seconds)			*Total Indentation Depth (Metres)*		
	Proposed Model		DIC Data	Proposed Model		DIC Data
	Method 1	Method 2	---	Method 1	Method 2	----
Exp 5	0.1196	0.1255	0.0730	0.3456	0.3076	0.1679
Exp 8	0.0969	0.1382	0.0947	0.3148	0.2709	0.2285

For experiment 8, and despite the very rough fits of the regression curves shown in Figure 4, the total time model shows very good agreement with the Method 1 derived parameters, with a roughly 2.3 percent increase in the model estimated collision times when compared to the DIC data. There is however a general overestimation of the indentation depth over the course of the impact, with the predicted maximum indentation depth being roughly 38 percent greater than the measured value. In contrast, use of the parameters derived from both methods for experiment 5 and from Method 2 for experiment 8 do not produce satisfactory results for either the total impact duration or indentation depth, where the modelled total times range from a 46% to a 72% increase when compared to the measured data. Of important note, one common point in all regressions that did not produce satisfactory results with the time history models is that the ice exponent, ex, was less than -1. These values are suspect as they result in impossible relationships between contact force and time, where the force trends towards infinity at the start of the collision. This is also the case for the force versus indentation depth relationship, where the contact force approaches infinity with the indentation depth approaching zero. Such unrealistic values also further call into question the suitability of the commonly used process-pressure area model for these impact scenarios.

The reason for such low ice exponent values for the spherical cap ice samples is twofold. First, use of this ice geometry results in very high peak loads near the start of the impacts (Andrade et al., 2025) after which major spalling of shattered ice occurs. Due to the ice expulsion after the initial peak load, there is a big discrepancy between the nominal and actual contact area, the former of which is much larger. This results in the calculation of very low nominal contact pressures as the collision progresses, demonstrated in Figure 4, affecting the parameters of the fitted power curve. This phenomenon may also account for why the model overestimates the ice indentation depth in Method 1 as lower nominal contact pressures result in softer ice. Second, the rapid increase in the nominal contact areas at the beginning of the impacts coupled with the fast rise in contact forces results in a significant portion of the nominal pressure-area data exhibiting a generally increasing trend, pushing the start of the subsequent decreasing pressure trend further from the point of zero contact when compared to data from conical ice samples. This also has consequences on the calculated curve fit parameters.

The differing behaviour of the indentation process between different ice geometries shown by Andrade et al. (2025) demonstrates some of the weaknesses of using a process pressure-area relationship defined in equation (2) to model the ice crushing strength of spherical cap shaped ice samples. This ice geometry approaches a flat-on-flat contact scenario, in contrast to impacts with conical samples beginning with a point contact, and as such the ice failure process differs significantly. This is illustrated by the differing force time histories between these two geometries, with the previously mentioned very high peak loads occurring early in impacts involving spherical cap shaped ice samples whereas conical ice samples are characterized by progressively growing impact forces being interrupted by multiple spalling events. Again, the process pressure-area is itself an idealization of the ice crushing process and may not be suitable for all ice collision scenarios. Despite this questionable suitability and the differing load history behaviour of spherical cap and the previous tested conical ice samples, the indentation-time model introduced in equation (8) produces adequate results if the ice exponent ex is greater than -1. Again, values greater than -1 correspond to force levels not trending to infinity at the start of the collision, instead starting at zero as expected. In addition, the total time model introduced in equation (10) produces remarkably accurate estimates for the impact durations. The lack of fit of the process pressure-area curves when compared to the relatively accurate model predictions may indicate that for the purposes of estimating specifically the total time

of a ship ice impact, the type of regression used is not of high importance and other regression models with simpler time derivations may be considered, though testing this is beyond the scope of the present study.

As such, use of the models for estimating the time history and total time of impacts between a rigid ship panel and spherical ice specimens is possible, but care should be taken when fitting a simple power curve to the nominal pressure-area data as the validity of these models for this impact scenario is questionable with very inexact regression fits. Collisions involving ice of this geometry tend to result in significant contact forces very early in the collision and this must be included in the development of any regressions even if the pressure data at this point does not follow an expected decreasing trend with increasing nominal contact area. Specifically, Method 1 as described previously should be used. Any fitted power curve should also be checked to ensure realistic contact force growth, with an ice exponent parameter, ex, of less than -1 possibly indicating an overstep in the applicability of the process pressure-area relationship defined in equation (2) to appropriately model the ice crushing strength of the impact.

CONCLUSIONS

This paper presents validation work towards an analytically derived time-history and total time models of a Popov-Daley style ship ice impact. Specifically, it uses experimental data from two large double pendulum ice impact experiments using spherical cap shaped ice indenters. The low fit power curve regression over the nominal pressure-data data call into question the applicability of the process pressure-area model for this type of impact scenario as the ice failure behaviour and force-time histories differ significantly when compared to conical ice samples. Despite this, the total time model produces acceptable results if the fitted power curve over the pressure-area data corresponds to a physically possible force-time history; if the ice exponent, ex, is greater than -1.

ACKNOWLEDGEMENTS

The authors graciously acknowledge the financial support from the NSERC DND/CRD [grant number DNDPJ 520471-17] “Operational Capabilities of Low- and Non-ice-class Structures in Ice” grant, and the following contributing project partners: Defence Research and Development Canada (Atlantic), Vard Marine Inc., the American Bureau of Shipping (ABS), and the Newfoundland & Labrador Provincial Government [grant number 5404-1984-102].

REFERENCES

Andrade, S.L., Gagnon, R.E., Quinton, B.W.T., 2025. A Follow-up on the Second Set of Ice Impact Experiments with the Large Double Pendulum Apparatus, in: Proceedings of the 28th International Conference on Port and Ocean Engineering under Arctic Conditions (POAC 2025). St. John’s, Newfoundland and Labrador, Canada.

Bryson, E.J.D., Andrade, S.L., Quinton, B.W.T., 2025. An Analytically Derived Solution for

the Time History of a Ship-Ice Impact (In Review). http://dx.doi.org/10.2139/ssrn.5165733
Daley, C., 2015. Ice Impact Capability of DRDC Notional Destroyer (DRDC Contract Report No. DRDC-RDDC-2015-C202). St. John's, Newfoundland and Labrador, Canada.
Daley, C., 2000. Background Notes to Design Ice Loads. IACS Ad-hoc Group on Polar Class Ships.
Daley, C., 1999. Energy Based Ice Collision Forces, in: Proceedings of the 15th International Conference on Port and Ocean Engineering under Arctic Conditions (POAC). Presented at the Port and Ocean Engineering under Arctic Conditions, POAC'99, Espoo, Finland, pp. 674–686.
Daley, C., Dolny, J., Daley, K., 2017. Safe Speed Assessment of DRDC Notional Destroyer in Ice (DRDC Contract Report No. DRDC-RDDC-2017-C259). St. John's, Newfoundland and Labrador, Canada.
Daley, C., Kim, H., 2010. Ice Collision Forces Considering Structural Deformation, in: Proceedings of the 29th International Conference on Ocean, Offshore and Arctic Engineering (OMAE). Presented at the OMAE 2010, American Society of Mechanical Engineers, Shanghai, China, pp. 817–825. https://doi.org/10.1115/OMAE2010-20657
Daley, C., Liu, J., 2010. Assessment of Ship Ice Loads in Pack Ice, in: 9th International Conference and Exhibition on Performance of Ships and Structures in Ice. SNAME, Anchorage, AK, USA. https://doi.org/10.5957/ICETECH-2010-141
Dolny, J., 2016. Methodology for Defining Technical Safe Speeds for Light Ice-Strengthened Government Vessels Operating in Ice (No. SSC-473). American Bureau of Shipping, Houston, Texas, USA.
Dolny, J.R., 2017. A Technical Methodology for Establishing Structural Limitations of Ships in Pack Ice (Master's Thesis). Memorial University of Newfoundland, St. John's, Newfoundland Labrador.
IACS, 2019. Requirements Concerning Polar Class. International Association of Classification Societies, London, UK.
Kim, E., Amdahl, J., 2016. Discussion of assumptions behind rule-based ice loads due to crushing. Ocean Engineering 119, 249–261. https://doi.org/10.1016/j.oceaneng.2015.09.034
Lande Andrade, S., Elruby, A., Oldford, D., Quinton, B., 2022. Assessing Polar Class Ship Overload and Ice Impact on Low-ice Class Vessels using a "Quasi Real Time" Popov/Daley Approach, in: Day 2 Wed, September 28, 2022. Presented at the SNAME Maritime Convention, SNAME, Houston, Texas, USA, p. D021S007R002. https://doi.org/10.5957/SMC-2022-108
National Institute of Standards and Technology, 2023. Digital Library of Mathematical Functions [WWW Document]. URL https://dlmf.nist.gov/15.4 (accessed 2.11.25).
Popov, Y., Faddeyev, O., Kheisin, D., Yalovlev, A., 1967. Strength of Ships Sailing in Ice (Translated) (No. FSTC-HT-23-96-68). Sudostroyeniye Publishing House, Leningrad, USSR. Translated by U.S. Army Foreign Science and Technology Center.
Riska, K., Kamarainen, J., 2012. Comparison of Finnish-Swedish and IACS Ice Class Rules, in: The International Conference on Ice Class Ships 2012. Presented at the The International Conference on Ice Class Ships 2012, RINA, pp. 43–62. https://doi.org/10.3940/rina.ice.2012.07